Characteristics of Nickel Ferrite Thin Film Magnetic Sensor Fabricated by Sputtering Technique

Ali S. Hashim, Basim K. Lateef

Department of Physics, College of Science, University of Samawa, Samawa, IRAQ

Abstract
In this work, a magnetic sensor was fabricated from nickel ferrite thin films prepared by sputtering technique. The nickel and iron targets were co-sputtered and the optimum samples were prepared using $Ar:O_2$ gas mixture of 40:60 mixing ratio, total gas pressure of 0.6 mbar, discharge voltage of 2.1 kV, discharge current of 20 mA and inter-electrode distance of 5 cm. These samples showed high structural purity and the minimum particle size was determined to be 25 nm. The average surface roughness of these samples was 0.465 nm. The sensor devices fabricated from these samples were characterized to determine the optimum preparation conditions and the minimum magnetic field intensity detected by the fabricated sensor was 38.2 G.

Keywords: Nickel ferrite; Magnetic sensor; Sputtering technique; Thin films
Received: 20 October 2023; **Revised:** 08 December; **Accepted:** 15 December; **Published:** 1 January 2024

1. Introduction

A sensor is a device that converts a physical phenomenon into an electrical signal. Such sensors represent part of the interface between the physical world and the electrical and electronic devices, such as control circuits and computers [1]. The highest quality, most up-to-date, most accurately calibrated and most carefully selected sensor can still give totally erroneous data if it is not correctly applied [2,3].

Magnetic sensors are widely used in the field of mineral, navigational, automotive, medical, industrial, military, and consumer electronics [4-7]. Many magnetic sensors have been developed that are generated by specific laws or phenomena: such as search-coil, fluxgate, Hall Effect, anisotropic magnetoresistance (AMR), giant magnetoresistance (GMR), magnetoelectric (ME), magnetodiode, magnetotransictor, fiber-optic, optical pump, superconducting quantum interference device (SQUID), etc. Each of these magnetic field sensors has their merits and application areas [8-10].

In the presence of an H field, the magnetic moments within a material tend to become aligned with the field and to reinforce it by virtue of their magnetic fields. The term $\mu_0 M$ in the equation above is a measure of this contribution. Magnetic susceptibilities up to 10^6 are possible for ferromagnetic materials.

Permanent magnetic moments in ferromagnetic materials result from atomic magnetic moments due to uncancelled electron spins as a consequence of the electron structure [11]. There is also an orbital magnetic moment contribution that is small in comparison to the spin moment. Furthermore, in a ferromagnetic material, coupling interactions cause net spin magnetic moments of adjacent atoms to align with one another, even in the absence of an external field [12]. All these features make these materials very important to respond to the magnetic fields in their environment as well as to detect magnetic materials [13]. Devices required for these purposes are known as magnetic sensors. These devices are designed and fabricated to detect as low as possible magnetic field strengths (H) and magnetization (M) [14].

2. Experimental Part

The dc plasma sputtering system used in this work contains of a vacuum chamber, two discharge electrodes, vacuum pumps and accessories, and cooling and heating facilities. The chamber could be evacuated

down to 10^{-3} mbar by a rotary pump and to 10^{-5} mbar by a diffusion pump. The base vacuum was determined by the purpose of the discharge process. Argon at maximum pressure of 0.6 mbar was used as the discharge gas and its pressure was finely controlled by needle valve. More details on the dc plasma sputtering system can be found in references [15,16].

The inter-electrode distance could be easily varied from 0 to 10cm as the system was operated. The cathode was cooled down to about 10°C to prevent the secondary electron emission while the anode could be heated by an underneath heater or kept at room temperature. The two targets of highly pure nickel (Ni, 0.9999) and iron (Fe, 0.999) were mounted on the cathode with some geometrical arrangement suitable for the work, while the glass substrate on which the films were deposited was placed on the anode. All results presented in this work were obtained by using the concentric arrangement of the Ni and Fe targets.

Highly-pure oxygen gas was flowing to the chamber throughout needle valve to represent the reactive gas required to form the compound of nickel ferrite. The mixture of argon and oxygen gases could be controlled by a gas mixing unit before entering the chamber.

The film thickness was measured by laser fringes method to be about 178nm for the sample prepared at 5 cm inter-electrode distance, 0.6 mbar gas pressure, 40:60 Ar:O_2 mixing ratio, 2.1 kV discharge voltage, 20 mA discharge current and deposition time of 4 hours.

The characterization and measurements included x-ray diffraction (XRD), scanning electron microscopy (SEM), atomic force microscopy (AFM) and Fourier-transform infrared (FTIR) spectroscopy. The magnetic measurements were carried out using an AlphLab GM-2 Gaussmeter.

The glass substrate - on which the 178nm $NiFe_2O_4$ thin film was deposited – was cut as a circle with 1cm diameter to represent the sensing part and be placed inside a metallic shield. The detected signal can be amplified by using a 2mm layer of Mn-doped SiC powder of 50μm grain size over the sensing film. The sensing part was maintained normally inside the metallic shield by epoxy. A disc of a magnetic insulating material with a center hole was used to confine the stainless steel screw that connecting the Mn-doped SiC layer to the Gaussmeter. All parts inside the shield were maintained by a hard plastic disc with a center hole to pass the screw. The screw was fastened by two nuts to represent the probe of the Gaussmeter.

The experimental measurements to detect the magnetic field near the fabricated sensor were carried out by using an experimental setup prepared in our lab as shown in the figure below. Two ring magnets each of 80mm outer diameter, 40mm inner diameter and 16mm thickness were used as the dc magnetic flux source. Therefore, a calibration process was performed for the magnetic field intensity with the distance from the magnet, which was placed on a scaled bench. The maximum value of magnetic flux density at the surface of the magnet (x=0) was 426.5G.

The standard probe of the Gaussmeter (Alpha Lab GM-2) was replaced by the fabricated sensors to test their response to the magnetic flux in their surroundings, as shown below. The readout of the Gaussmeter using the standard probe was recorded at different distances from the magnetic field source to be 54.5G at a point P1 in the figure. At the same point, the readout of the Gaussmeter using the fabricated sensor was also recorded to be 38.2G.

Nanopowder sensor exhibits higher values of detected magnetic field than the thin film sensor. However, the fluctuations in readouts from the nanopowder sensor forced us to use and enhance the thin film sensor design.

3. Results and Discussion

Figure (1) shows a photograph of the $NiFe_2O_4$ thin films prepared in this work on glass substrates using argon and oxygen gas mixture of 40:60 mixing ratio at different

inter-electrode distances (2-6cm). The samples prepared at inter-electrode distance of 5cm (second from left) showed the highest homogeneity in the film thickness. Therefore, they were selected to fabricate the magnetic sensor device.

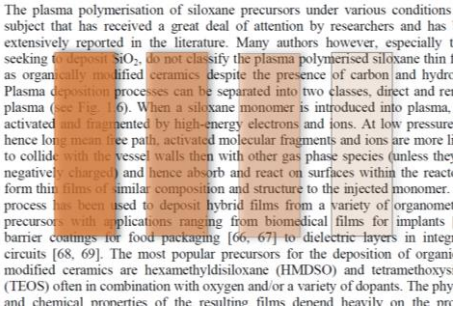
The plasma polymerisation of siloxane precursors under various conditions subject that has received a great deal of attention by researchers and has extensively reported in the literature. Many authors however, especially t seeking to deposit SiO_2, do not classify the plasma polymerised siloxane thin f as organically modified ceramics despite the presence of carbon and hydr Plasma deposition processes can be separated into two classes, direct and re plasma (see Fig. 1.6). When a siloxane monomer is introduced into plasma, activated and fragmented by high-energy electrons and ions. At low pressure hence long mean free path, activated molecular fragments and ions are more li to collide with the vessel walls then with other gas phase species (unless they negatively charged) and hence absorb and react on surfaces within the reacto form thin films of similar composition and structure to the injected monomer. process has been used to deposit hybrid films from a variety of organomet precursors with applications ranging from biomedical films for implants barrier coatings for food packaging [66, 67] to dielectric layers in integ circuits [68, 69]. The most popular precursors for the deposition of organi modified ceramics are hexamethyldisiloxane (HMDSO) and tetramethoxys (TEOS) often in combination with oxygen and/or a variety of dopants. The phy and chemical properties of the resulting films depend heavily on the pro

Fig. (1) The $NiFe_2O_4$ thin film samples prepared on glass substrates at different inter-electrode distances using $Ar:O_2$ gas mixture of 40:60 mixing ratio

Figure (2) shows the XRD pattern of the $NiFe_2O_4$ thin film sample prepared at inter-electrode distance of 5cm using $Ar:O_2$ gas mixture of 40:60 mixing ratio. The structure of the sample was determined to be polycrystalline and sharp peaks are observed at diffraction angles of 30.10°, 35.51°, 43.16°, 56.96°, 57.15° and 62.74°. These angles correspond to crystal planes of (220), (311), (400), (422), (511) and (440), respectively. The most dominant crystalline orientation is (311) with approximate grain size of 13nm.

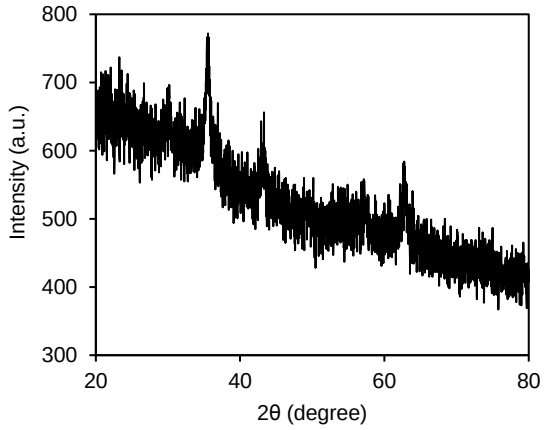

Fig. (2) The XRD pattern of the $NiFe_2O_4$ thin film sample prepared at inter-electrode distance of 4cm using $Ar:O_2$ gas mixture of 30:70 mixing ratio

As for most sensing device applications, the surface area is required to be as large as possible, nanostructures are principally satisfying this requirement with surface roughness lower than 5nm. The 3D AFM image of the prepared surface is shown in Fig. (3) and the average roughness is determined to be 0.465nm. Such value can reasonably improve the sensitivity of the prepared surface to the surrounding magnetic fields.

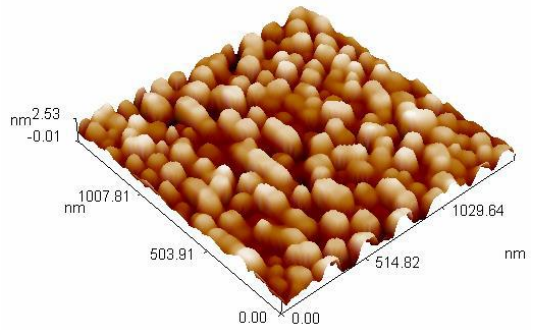

Fig. (3) The 3D AFM image of the $NiFe_2O_4$ thin film sample prepared at inter-electrode distance of 4cm using $Ar:O_2$ gas mixture of 30:70 mixing ratio

Figure (4) shows the response of the fabricated thin film sensor as a function of distance from the magnetic flux source. At distances shorter than 15cm from the source, the sensor has detected flux density of 24-80% of the values measured by using the standard probe of the Gaussmeter. At longer distances, the measurements were comparable to those measured before.

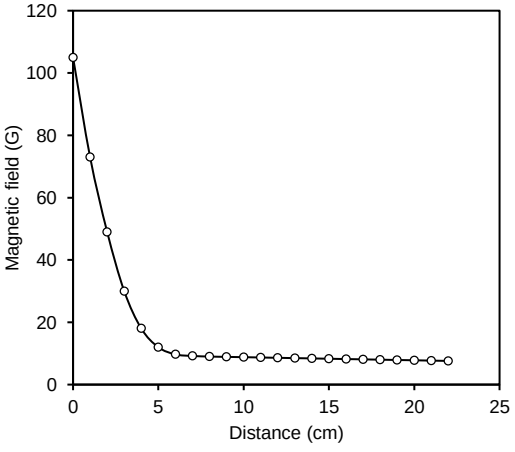

Fig. (4) The response of the fabricated thin film sensor as a function of distance from the magnetic flux source

With repeated measurements using the fabricated sensor, it showed sufficient

stability in the measured flux densities. Therefore, the $NiFe_2O_4$ thin film magnetic sensor fabricated in this work can be good attempt to produce reliable device for different applications of magnetics and magnetic field detectors. The compact sensor is shown in Fig. (5).

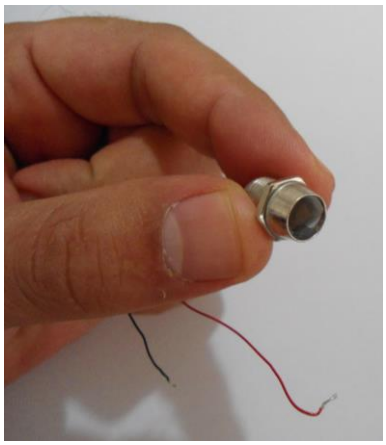

Fig. (5) Final compact assembly of the nanostructured $NiFe_2O_4$ thin film magnetic sensor fabricated in this work

4. Conclusions

In concluding remarks, a dc reactive co-sputtering technique was used to prepare nanostructured nickel ferrite thin films on glass substrates. Highly-pure polycrystalline structures with dominant orientation in the (311) plane, minimum nanoparticle size of 25nm, and average roughness of 0.465nm were prepared. Minimum magnetic flux density of 38.2G was measured by the fabricated device as a magnetic sensor. This device exhibits high reliability, low production cost and excellent mechanical rigidity to satisfy the outdoor and industrial uses of such devices.

References

[1] S. Shen, J. Chen, M. Wang, X. Sheng, X. Chen, X. Feng and S.S. Mao, "Titanium dioxide nanostructures for photoelectrochemical applications", Prog. In Mater. Sci., 98 (2018) 299-385.

[2] E.A. Al-Oubidy and F.J. Kadhim, "Photocatalytic activity of anatase titanium dioxide nanostructures prepared by reactive magnetron sputtering technique", Opt. Quantum Electron., 51(1) (2019) 23.

[3] K. Vidhya, M. Saravanan, G. Bhoopathi, V.P. Devarajan and S. Subanya, "Structural and optical characterization of pure and starch-capped ZnO quantum dots and their photocatalytic activity", Appl. Nanosci., 5 (2015) 235-243.

[4] K. Kim, M.-J. Kim, S.-I. Kim and J.-H. Jang, "Towards visible light hydrogen generation: quantum dot-sensitization via efficient light harvesting of hybrid-TiO_2", Sci. Rep., 3 (2013) 1-8.

[5] D. Wu, S. Zhang, S. Jiang, J. He and K. Jiang, "Anatase TiO_2 hierarchical structures composed of ultra-thin nano-sheets exposing high percentage {001} facets and their application in quantum-dot sensitized solar cells", J. Alloys Compd., 624 (2015) 94-99.

[6] H.A. Alhadrami, A. Baqasi, J. Iqbal, R.A.M. Shoudri, A.M. Ashshi, E.I. Azhar, F. Al-Hazmi, A. Al-Ghamdi and S. Wageh, "Antibacterial Applications of Anatase TiO_2 Nanoparticle", Am. J. Nanomater., 5(1) (2017) 31-42.

[7] M.T. Noman, M.A. Ashraf and A. Ali, "Synthesis and applications of nano-TiO_2: a review", Environ. Sci. Pollut. Res., 26 (2019) 3262-3291.

[8] O.A. Hammadi, "Production of Nanopowders from Physical Vapor Deposited Films on Nonmetallic Substrates by Conjunctional Freezing-Assisted Ultrasonic Extraction Method", Proc. IMechE, Part N, J. Nanomater. Nanoeng. Nanosys., 232(4) (2018) 135-140.

[9] O.A. Hammadi, M.K. Khalaf, F.J. Kadhim, "Fabrication of UV Photodetector from Nickel Oxide Nanoparticles Deposited on Silicon Substrate by Closed-Field Unbalanced Dual Magnetron Sputtering Techniques", Opt. Quantum Electron., 47(12) (2015) 3805-3813.

[10] O.A. Hammadi, M.K. Khalaf, F.J. Kadhim, "Silicon Nitride Nanostructures Prepared by Reactive Sputtering Using Closed-Field Unbalanced Dual Magnetrons", Proc. IMechE, Part L, J. Mater.: Design and Applications, 231(5) (2017) 479-487.

[11] M.A. Hameed and Z.M. Jabbar, "Optimization of Preparation Conditions to Control Structural Characteristics of Silicon Dioxide Nanostructures Prepared by Magnetron Plasma Sputtering", Silicon, 10(4) (2018) 1411-1418.

[12] F.J. Al-Maliki, O.A. Hammadi and E.A. Al-Oubidy, "Optimization of Rutile/Anatase Ratio in Titanium Dioxide Nanostructures prepared by DC Magnetron Sputtering Technique", Iraqi J. Sci., 60 (2019) 91-98.

[13] O.A. Hammadi, F.J. Al-Maliki and E.A. Al-Oubidy, "Photocatalytic Activity of Nitrogen-Doped Titanium Dioxide Nanostructures Synthesized by DC Reactive Magnetron Sputtering Technique", Nonlinear Opt. Quantum Opt., 51 (1-2) (2019) 67-78.

[14] O.A. Hammadi, M.K. Khalaf, F.J. Kadhim, B.T. Chiad, "Operation Characteristics of a Closed-Field Unbalanced Dual-Magnetrons Plasma Sputtering System", Bulg. J. Phys., 41(1) (2014) 24-33.

[15] O.A. Hammadi, M.K. Khalaf, F.J. Kadhim, "Fabrication and Characterization of UV Photodetectors Based on Silicon Nitride Nanostructures Prepared by Magnetron Sputtering", Proc. IMechE, Part N, J. Nanoeng. Nanosys., 230(1) (2016) 32-36.

[16] O.A. Hammadi and N.E. Naji, "Characterization of Polycrystalline Nickel Cobaltite Nanostructures Prepared by DC Plasma Magnetron Co-Sputtering for Gas Sensing Applications", Photon. Sens., 8(1) (2018) 43-47.

